

AD-760 766

ELASTIC PROPERTIES OF OXIDES AND THE
SEARCH FOR TEMPERATURE-COMPENSATED
MATERIALS

R. E. Newnham

Pennsylvania State University

Prepared for:

Air Force Cambridge Research Laboratories

30 March 1973

DISTRIBUTED BY:

NTIS

National Technical Information Service
U. S. DEPARTMENT OF COMMERCE
5285 Port Royal Road, Springfield Va. 22151

ELASTIC PROPERTIES OF OXIDES AND THE SEARCH
FOR TEMPERATURE-COMPENSATED MATERIALS

by
R.E. Newnham

Materials Research Laboratory
The Pennsylvania State University
University Park, Pennsylvania, 16902

Contract No. FI9628-73-C-0108
Project No. 5635
Task No. 563503
Work Unit No. 56350301

Scientific Report No. 1.

March 30, 1973

Contract Monitor: Paul H. Carr
Microwave Physics Laboratory

Approved for public release; distribution unlimited.

Prepared
for

Air Force Cambridge Research Laboratories
Air Force Systems Command
United States Air Force
Bedford, Massachusetts
01730

Reproduced by
NATIONAL TECHNICAL
INFORMATION SERVICE
U S Department of Commerce
Springfield VA 22131

D D C
RECEIVED
JUN 7 1973
RECEIVED
B

ACCESSION for		
ITIS	White Section	<input checked="" type="checkbox"/>
" 2	Buff Section	<input type="checkbox"/>
UNAN. CHNGED		<input type="checkbox"/>
CLASSIFICATION		
BY		
DISTRIBUTION/AVAILABILITY CODES		
BIBL.	AVAIL. and/or	SPECIAL
A		

Qualified requestors may obtain additional copies from the Defense Documentation Center. All others should apply to the National Technical Information Service.

ABSTRACT

New temperature-compensated high piezoelectric coupling crystals are needed for acoustic surface-wave matched filters, encoders, decoders, and related signal processing devices. Elastic coefficients, together with their pressure and temperature derivatives, are also important in materials science and in geophysics. Oxides show several correlations between structure type and elastic behavior. Stiffness coefficients of silicate minerals are generally larger in the direction of Si-O bonding. A simple mechanical analogy in which atomic bonds are simulated by springs connected in series and parallel is used to estimate the size and anisotropy of the elastic moduli. Magnitudes of the temperature and pressure derivatives of the stiffness coefficients are also predicted by the model. Crystallochemical factors conducive to anomalous elastic behavior are examined, with special attention to materials which become stiffer with increasing temperature. Internal rotational motions involving bending of the atomic bonds appear particularly important in this class of materials.

ie

DOCUMENT CONTROL DATA - R&D

(Security classification of title, body of abstract and indexing annotation must be entered when the overall report is classified)

1. ORIGINATING ACTIVITY (Corporate author) The Pennsylvania State University Materials Research Laboratory University Park, Pennsylvania 16802		2a. REPORT SECURITY CLASSIFICATION Unclassified	
		2b. GROUP	
3. REPORT TITLE ELASTIC PROPERTIES OF OXIDES AND THE SEARCH FOR TEMPERATURE-COMPENSATED MATERIALS			
4. DESCRIPTIVE NOTES (Type of report and inclusive dates) Scientific. Interim.			
5. AUTHOR(S) (First name, middle initial, last name) R. E. Newnham			
6. REPORT DATE 30 March 1973		7a. TOTAL NO. OF PAGES 28 32	7b. NO. OF REFS 19
8a. CONTRACT OR GRANT NO. F19628-73-C-0108		9a. ORIGINATOR'S REPORT NUMBER(S) Scientific Report No. 1	
a. PROJECT, TASK, WORK UNIT NOS. 5635-03-01			
c. DOD ELEMENT 61102F		9b. OTHER REPORT NO(S) (Any other numbers that may be assigned this report)	
d. DOD SUBELEMENT 681305		AFCRL-TR-73-0220	
10. DISTRIBUTION STATEMENT A - Approved for public release; distribution unlimited.			
11. SUPPLEMENTARY NOTES TECH, OTHER		12. SPONSORING MILITARY ACTIVITY Air Force Cambridge Research Laboratories (L2) L. G. Hanscom Field Bedford, Massachusetts 01730	

New temperature-compensated high piezoelectric coupling crystals are needed for acoustic surface-wave matched filters, encoders, decoders, and related signal processing devices. Elastic coefficients, together with their pressure and temperature derivatives, are also important in materials science and in geophysics. Oxides show several correlations between structure type and elastic behavior. Stiffness coefficients of silicate minerals are generally larger in the direction of Si-O bonding. A simple mechanical analogy in which atomic bonds are simulated by springs connected in series and parallel is used to estimate the size and anisotropy of the elastic moduli. Magnitudes of the temperature and pressure derivatives of the stiffness coefficients are also predicted by the model. Crystallochemical factors conducive to anomalous elastic behavior are examined, with special attention to materials which become stiffer with increasing temperature. Internal rotational motions involving bending of the atomic bonds appear particularly important in this class of materials.

Unclassified

Security Classification

14.	KEY WORDS	LINK A		LINK B		LINK C	
		ROLE	WT	ROLE	WT	ROLE	WT
	ELASTIC PROPERTIES TEMPERATURE-COMPENSATED MATERIALS OXIDES STIFFNESS COEFFICIENTS						

ELASTIC PROPERTIES OF OXIDES AND THE SEARCH FOR TEMPERATURE-COMPENSATED MATERIALS

R. E. Newnham
Materials Research Laboratory
The Pennsylvania State University

INTRODUCTION

Recent development of acousto-optic and surface-wave devices has renewed interest in the elastic properties of oxides. New temperature-compensated materials with large piezoelectric moduli are especially needed. In a delay-line medium, an electric signal is converted to an acoustic wave which travels at a slower velocity and is subsequently re-converted to an electric signal. Elastic coefficients govern the velocity of the acoustic wave, and hence the transit time.

Elastic properties of oxides are also important in the geosciences, since most minerals in the earth's crust are oxides. Stiffness moduli bear special relevance to our understanding of rock mechanics and seismic wave velocities.

From previous work it appears that packing density is the primary variable affecting the elastic moduli of oxide compounds. Birch (1961a, 1961b) showed that most common minerals have about the same mean atomic weight (molecular weight divided by the number of atoms in the chemical formula), and that

longitudinal sound velocity is roughly proportional to density. Shear velocities also increase with rock density (Simmons, 1964). Anderson and Nafe (1965) plotted bulk modulus (reciprocal volume compressibility) against volume per ion pair, demonstrating that most oxide data follow the same relation. Bulk modulus is inversely proportional to volume, regardless of whether the volume change is caused by pressure, compositional variation, temperature, porosity, or phase changes. As might be expected, bulk modulus increases with density because short-range repulsive forces make it increasingly difficult to compress the solid as the atoms move closer together.

STRUCTURE-STIFFNESS CORRELATION

All solids change shape under forces. Under small stress, the strain ϵ is related to the stress σ by Hooke's law, $(\sigma) = (c)(\epsilon)$. The elastic stiffness coefficients (c) constitute a fourth rank tensor in which the number of independent coefficients depends on symmetry (Nye, 1957). In contracted matrix notation $\sigma_i = c_{ij}\epsilon_j$ where $i, j = 1, 2, 3$ refer to longitudinal stresses and strains along axes X_1, X_2 and X_3 , respectively. For shearing motions about each of the axes, $i, j = 4, 5, 6$. The discussion which follows will be concerned with the relative values of c_{11}, c_{22} and c_{33} , the coefficients relating change in length along a principal direction to a parallel component of stress.

The stiffness coefficients for silicate minerals presented in Table 1 show a correlation between elastic anisotropy and structure type. All silicates contain (SiO_4) tetrahedra and, depending on how the tetrahedra are linked together, can be classified as framework, layer, chain or ring silicates.

In framework silicates such as quartz and silica glass, the tetrahedra form three-dimensional networks. Since the bonding is nearly isotropic, there is no cleavage and little anisotropy in hardness or elasticity. Compare the

Table 1

Longitudinal Stiffness Constants Expressed in Megabars (HEARNON, 1966)

Framework Silicates

α -quartz	SiO_2	$c_{11} = c_{22} = 0.9, c_{33} = 1.1$
silica glass	SiO_2	$c_{11} = c_{22} = c_{33} = 0.8$

Single Chain Silicates (pyroxenes)

aegerine	$\text{NaFeSi}_2\text{O}_6$	$c_{11} = 1.9, c_{22} = 1.8, c_{33} = 2.3$
augite	$(\text{CaMgFe})\text{SiO}_3$	$c_{11} = 1.8, c_{22} = 1.5, c_{33} = 2.2$
diopside	$\text{CaMgSi}_2\text{O}_6$	$c_{11} = 2.0, c_{22} = 1.8, c_{33} = 2.4$

Double Chain Silicates (amphiboles)

hornblende	$(\text{Ca,Na,K})_{2-3}(\text{Mg,Fe,Al})_5(\text{Si,Al})_8\text{O}_{22}(\text{OH})_2$	$c_{11} = 1.2, c_{22} = 1.8, c_{33} = 2.0$
------------	---	--

Ring Silicates

beryl	$\text{Be}_3\text{Al}_2\text{Si}_6\text{O}_{18}$	$c_{11} = c_{22} = 3.1, c_{33} = 2.8$
tourmaline	$(\text{Na,Ca})(\text{Li,Mg,Al})_3(\text{Al,Fe,Mn})_6(\text{OH})_4(\text{BO}_3)_3\text{Si}_6\text{O}_{18}$	$c_{11} = c_{22} = 2.7, c_{33} = 1.6$

Layer Silicates

biotite	$\text{K}(\text{Mg,Fe})_3(\text{AlSi}_3\text{O}_{10})(\text{OH})_2$	$c_{11} = c_{22} = 1.9, c_{33} = 0.5$
muscovite	$\text{KAl}_2(\text{AlSi}_3\text{O}_{10})(\text{OH})_2$	$c_{11} = c_{22} = 1.8, c_{33} = 0.6$
phlogopite	$\text{KMg}_3(\text{AlSi}_3\text{O}_{10})(\text{OH})_2$	$c_{11} = c_{22} = 1.8, c_{33} = 0.5$

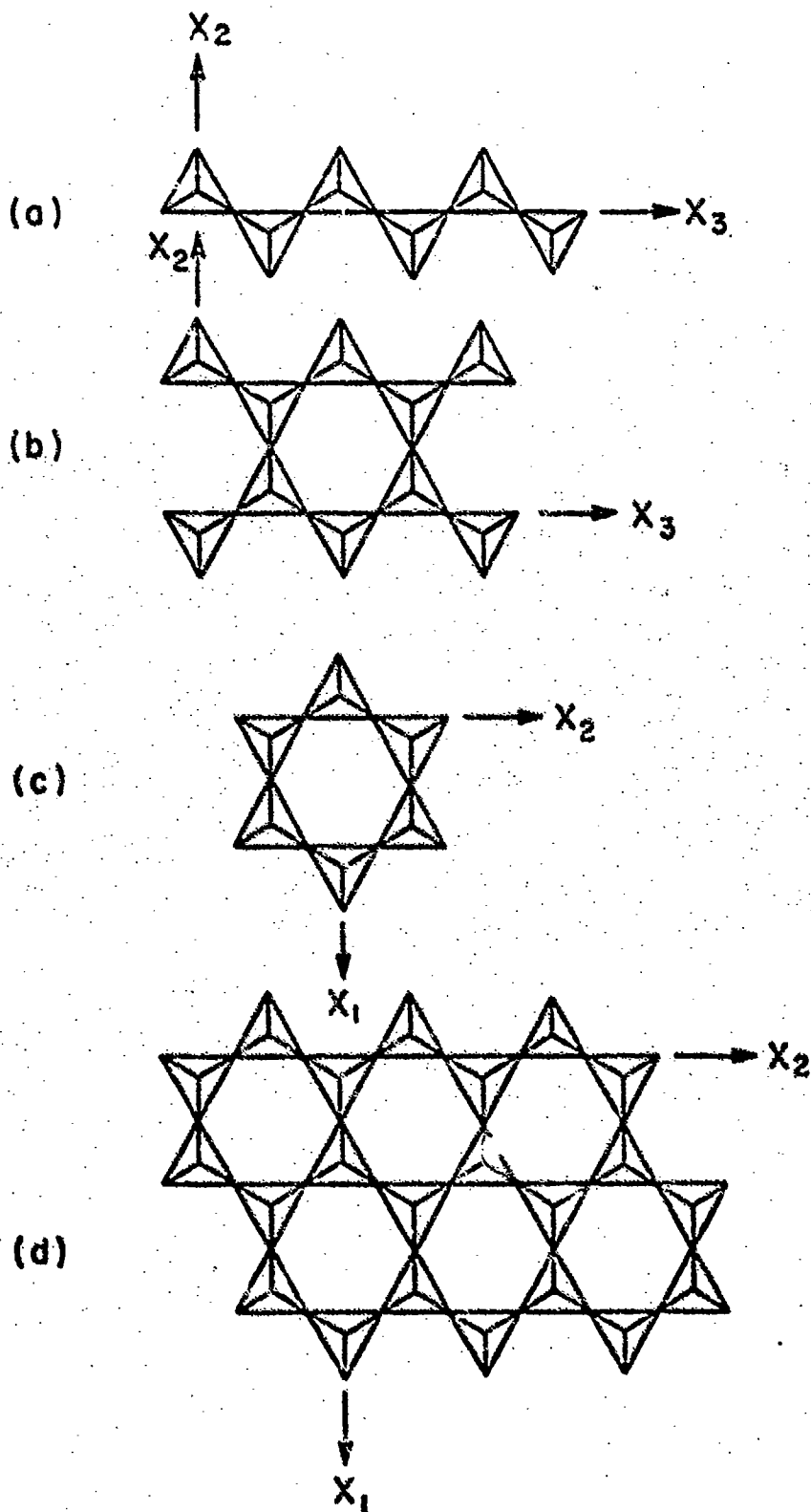
longitudinal elastic moduli given in Table 1. When corrected for density ($\rho = 2.65$ gms/c.c. for quartz and 2.2 gms/c.c. for silica glass) the stiffness constants are nearly identical for the two forms of SiO_2 , substantiating the relation between bulk modulus and volume (Anderson and Nafe, 1965).

The influence of crystal structure becomes more obvious in the chain silicates. Pyroxenes contain SiO_3 single chains, and amphiboles Si_4O_{11} double chains as shown in Fig. 1. Elastic coefficients in Table 1 are referred to the measurement directions denoted by arrows in Fig. 1. Bonding is stronger along the chain direction giving rise to pronounced cleavage. We also expect the crystal to be stiffer in this direction, resulting in larger moduli. Experiment confirms this suggestion; the stiffness parallel to the chain (c_{33}) is the largest in pyroxenes and amphiboles. We also note that c_{22} has increased considerably in hornblende, possibly because of the increase of chain width in this direction.

Beryl and tourmaline, two ring silicates, show a similar correlation between stiffness and structure. Both contain Si_6O_{18} rings as illustrated schematically in Fig. 1. We expect strong bonding and greater stiffness in the plane of the ring, hence c_{33} should be smaller than c_{11} and c_{22} as observed. Beryl is not very anisotropic because of the strong Be-O and Al-O bonds connecting the rings.

When Si_6O_{18} rings adjoin one another, the tetrahedral layer found in micas is formed. The cleavage and stiffness anisotropy become very obvious in layer silicates, where c_{11} and c_{22} are three times larger than c_{33} . This is the maximum elastic anisotropy observed, for reasons that are explained later.

Fig. 1. Arrangements of SiO_4 tetrahedra in silicates.
 (a) Single chain silicates. (b) Double chain silicates. (c) Ring silicates. (d) Layer silicates.



MECHANICAL ANALOG

In the lattice theory of elastic coefficients, stiffness coefficients are related to atomic force constants by determining the energy associated with various strain components. The calculation is cumbersome for a monatomic simple cubic lattice (Kittel, 1953), and would be overwhelming for most mineral structures. To avoid mathematical complexity and gain further physical insight regarding the causes of elastic anisotropy, we make use of a simple mechanical system.

The analogy used to describe elastic anisotropy is one in which two mechanical springs represent atomic bonds with force constants k and K . Tables of force constants (Wilson, Decius and Cross, 1955) derived from infrared vibrational spectra show that typical values are within an order of magnitude of 10^5 dynes/cm (1 md/Å). Stretching force constants are plotted as a function of interatomic distance in Fig. 2. As might be expected, the force constant decreases with increasing bond length, though it is rather surprising that so many different types fall along the same line. In general the strongest bonds have the largest force constants because deep potential wells have larger second derivatives when well-shapes are similar. Thus, for example, it is found that the stretching force constants for C-C, C=C, and C≡C are about 5, 10 and 16 md/Å, respectively. For bending motions, the force constants lie in the range 0.1 - 0.8 md/Å. Bending force constants are much smaller than stretching force constants because the repulsive overlap potential dominates when atoms move toward one another, increasing the force constant for stretching motion.

To explain the elastic properties of solids containing both strong and weak bonds, consider the spring systems illustrated in Fig. 3. When strong and weak springs are connected in series, most of the elastic energy is stored in the weak springs, while in the parallel connection the strong spring

Fig. 2. Relationship between force constant and interatomic distance. Stretching force constants are from Wilson Decius and Cross (1955), and interatomic distances from Sutton (1958).

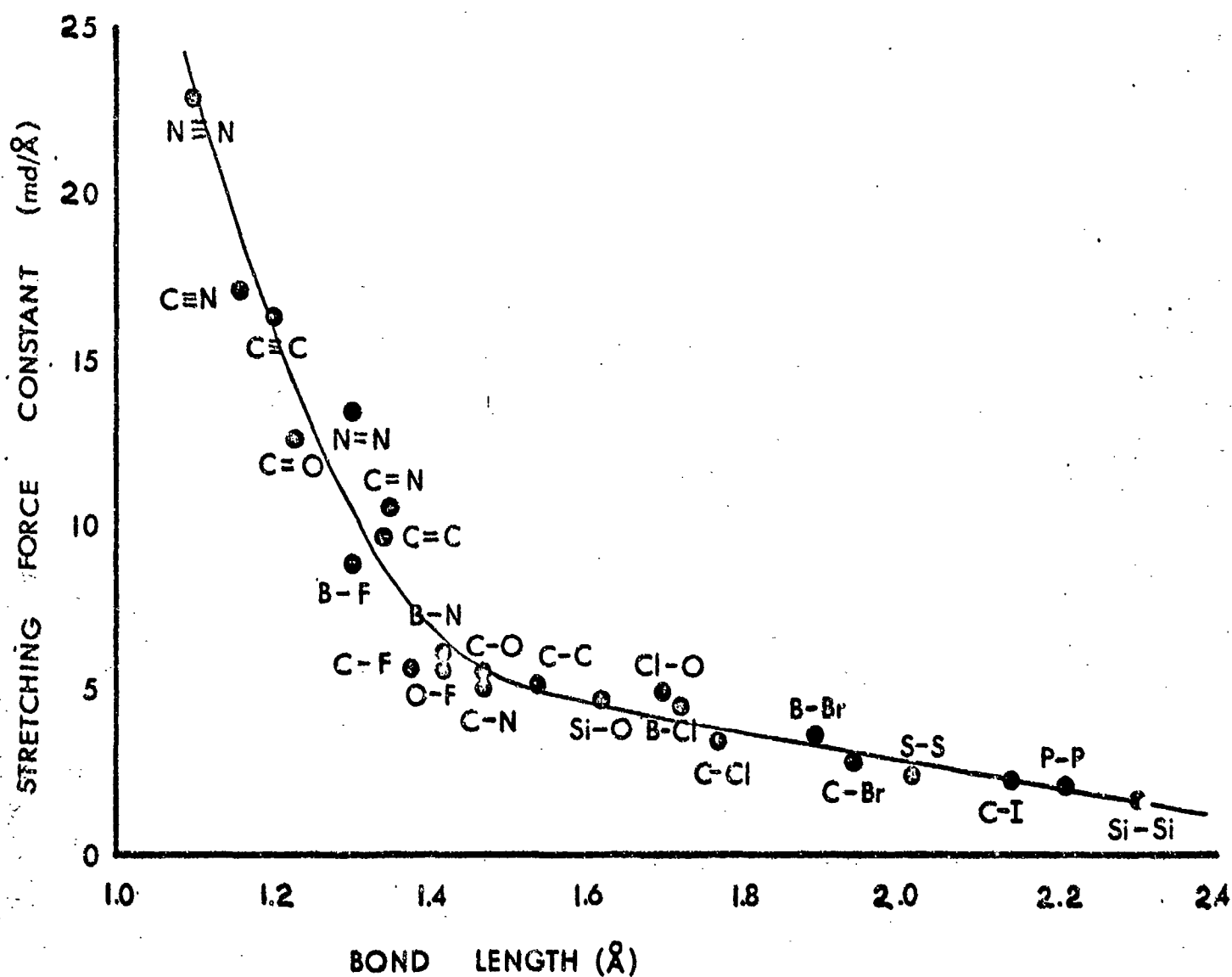
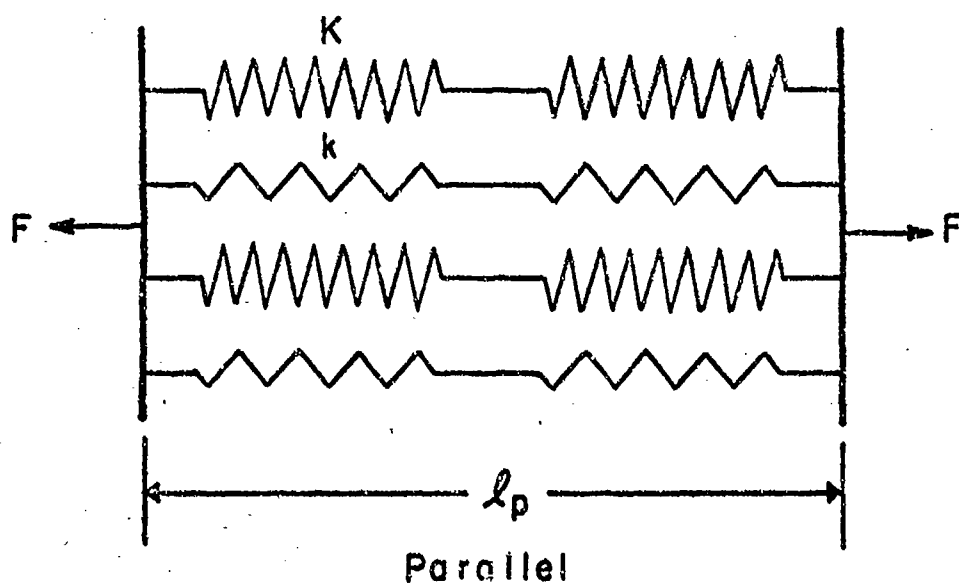
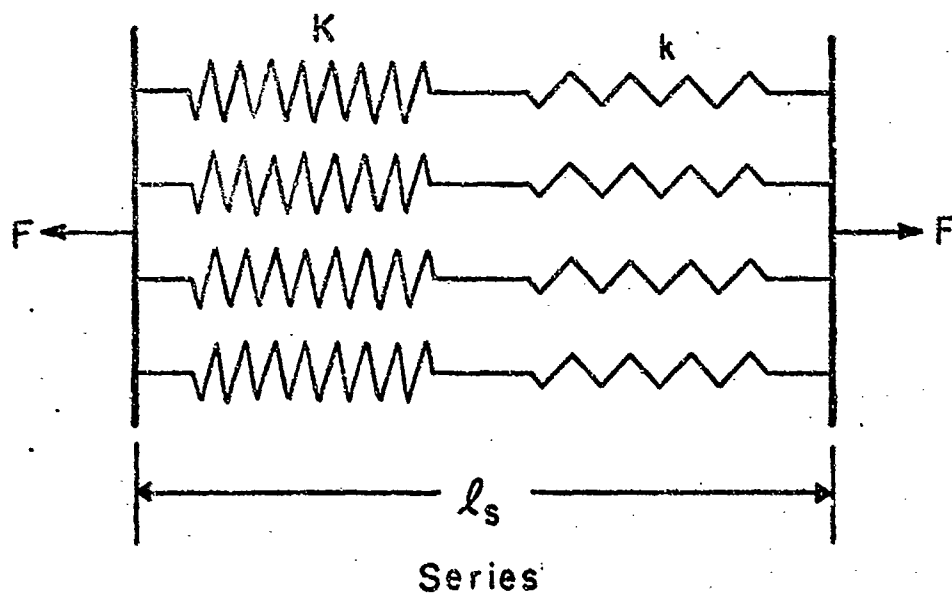


Fig. 3. Series and parallel connections of springs used to represent atomic bonds. Strong bonds have large force constants K , while weak bonds are easily stretched and have smaller constants k .



contains most of the energy. Let K and k be the force constants of two bonds arranged in series and parallel positions, as shown. This is a schematic representation of the bonding in mica. In muscovite Si-O and K-O bonds are in series for tensile stresses applied perpendicular to the sheet and in parallel when the applied forces lie in the plane. In pyroxenes, the parallel connection applies to measurements along the silicate chains, and series connections to the two perpendicular direction.

Analyzing the series arrangement for an applied tensile force F gives $F = \sigma A_s = n_s K u_K + n_s k u_k = c_s A_s u_s / \ell_s$ where σ is the stress acting on a surface of cross-sectional area A_s containing n_s chains, u_s / ℓ_s is the resulting strain in the series (s) connection whose overall stiffness is c_s . u_K and u_k are the displacements of the springs with force constants K and k . An identical force applied to the parallel arrangement gives an analogous expression. $F = \sigma A_p = n_p K u_K + n_p k u_k = c_p A_p u_p / \ell_p$. For the series connection both springs experience the same force so that their restoring forces are equal, $u_K K = u_k k$. The total displacement $u_s = u_k + u_K$, giving $u_k = u_s / (1 + k/K)$ and $u_K = u_s / (1 + K/k)$, and

$$c_s = \frac{n_s \ell_s}{A_s} \left(\frac{2kK}{k+K} \right) \quad (1)$$

In solving the parallel chain system, it is obvious that the displacements of the different springs are equal and that $u_p = 2u_k = 2u_K$. Substitution in the force equation gives the elastic constant

$$c_p = \frac{n_p \ell_p}{A_p} \left(\frac{k+K}{2} \right) \quad (2)$$

Note that c_s and c_p are unequal, even when all the springs are identical ($k = K$). The elastic coefficients depend on bond lengths through ℓ and on the number of chains per unit area in different directions.

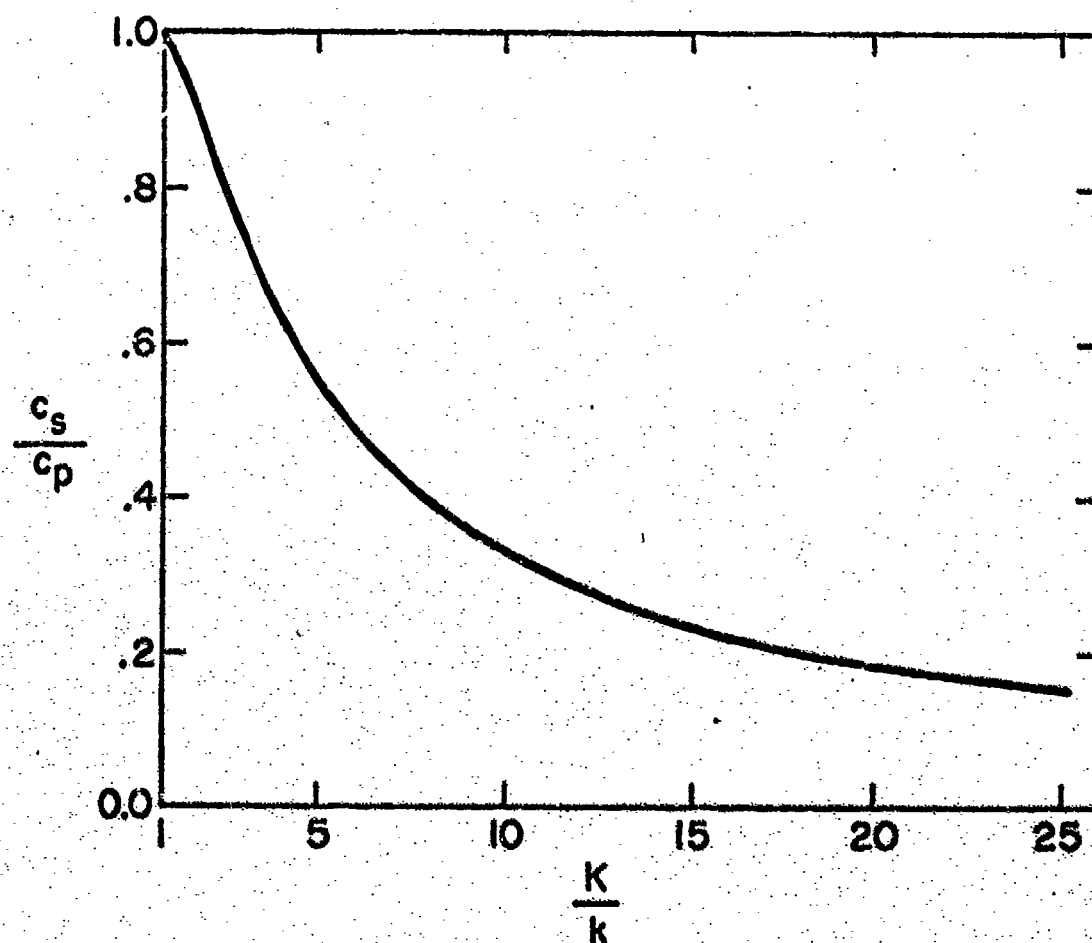
To determine the effects of strong and weak bonding on the elastic constants, assume that the geometric factors are about equal so that $n_p \ell_p / A_p$ $n_s \ell_s / A_s$, giving the ratio $c_s / c_p = 4kK / (k+K)^2$. In Fig. 4, the quantity c_s / c_p is plotted as a function of K/k to illustrate the effects of mixed bonding. When $K/k = 1$, all bonds have the same force constant, and the elastic constants are of course the same for series and parallel connection, so that $c_s / c_p = 1$. At the other extreme $c_s / c_p \rightarrow 0$ as $K/k \rightarrow \infty$, but the approach to zero is very slow. For $K/k = 2$, $c_s = 0.9c_p$ and even for $K/k = 10$, $c_s = 0.3c_p$. Since force constants for various chemical bonds are all within an order of magnitude of one another, the expected maximum elastic anisotropy is about 3:1, as observed in muscovite (Table 1). In all cases $c_p > c_s$ as observed experimentally.

It would be useful to predict the magnitude of the observed stiffness coefficients (Table 1) as well as their anisotropy. For chains identical in size, number and force constants, equations (1) and (2) reduce to

$$c_p = c_s = \frac{n\ell}{A} k, \quad (3)$$

n , ℓ , and A can be evaluated from the crystal structure, but k cannot. Typical values for k are 0.1 to 1.0 millidynes/Å for bending force constants and 1-10 md/Å for stretching constants. Both types of deformation come into play in minerals. When an SiO_4 tetrahedron is stressed, for instance both stretching and bending will take place. Si-O force constants (Matossi, 1949) are fairly typical with stretching constants 4-5 md/Å and bending constants 0.6 to 0.9 md/Å, while those involving Al are 10-20% smaller (Hidalgo and Serratos, 1956). A careful analysis would be required to determine the correct force constant to

Fig. 4. Stiffness anisotropy for series and parallel connections plotted as a function of spring constant ratio K/k . The series connection is far more pliant when $K \gg k$.



use in (3), but in any case all the atomic force constants have not been determined from spectroscopic data. When an average value $k \sim 1 \text{ md}/\text{\AA}$ is substituted in (3), elastic stiffness coefficients of the right magnitude are obtained. Taking $\ell \sim 3\text{\AA}$, $\frac{n}{A} \sim 1/\ell^2 \sim 0.1\text{\AA}^{-2}$ gives $c \sim 3 \times 10^{12} \frac{\text{dynes}}{\text{cm}^2} = 3 \text{ megabars}$, comparable to the experimental values (Table 1).

PRESSURE DEPENDENCE OF THE ELASTIC STIFFNESS

The pressure derivatives of the elastic coefficients of minerals determine changes in seismic wave velocities deep within the earth, and are strong indicators of the onset of phase transformation. Elastic stiffness coefficients and their initial pressure derivatives for four oxides are listed in Table 2.

Using the spring model just described, three observations are to be rationalized:

- (1) The pressure derivatives are all about one to ten megabar/megabar. (dimensionless).
- (2) Large stiffnesses usually show greater pressure derivatives than small ones: if $c_{11} > c_{22}$, then $\frac{\partial c_{11}}{\partial P} > \frac{\partial c_{22}}{\partial P}$.
- (3) Pressure derivatives of the stiffnesses are positive in dense-packed structures but in open structures are occasionally negative. Quartz and beryl each have one negative derivative but the close-packed corundum and forsterite structures show none.

To estimate the pressure dependence of the elastic stiffness we again make the approximation that $n/A \sim 1/\ell^2$, then $c = k/\ell$, and

$$\Delta c / \Delta P = (1/\ell) (\Delta k / \Delta P) - (k/\ell^2) (\Delta \ell / \Delta P). \text{ Assuming an isotropic solid, } \Delta P \sim (\Delta \ell) (c/\ell)$$

so that

$$\frac{\Delta c}{\Delta P} = -\frac{1}{c} \frac{\Delta k}{\Delta \ell} + \frac{k}{\ell c} \quad (2)$$

Comparison of elastic stiffness and their initial pressure derivatives for four oxides. Adiabatic stiffness c_{ij} are expressed in megabars, and the pressure derivatives $\partial c_{ij}/\partial P$ are dimensionless.

	Beryl		Quartz		Corundum		Forsterite	
ij	c_{ij}	$\partial c_{ij}/\partial P$	c_{ij}	$\partial c_{ij}/\partial P$	c_{ij}	$\partial c_{ij}/\partial P$	c_{ij}	$\partial c_{ij}/\partial P$
11	3.09	4.5	0.87	3.3	4.98	6.2	3.29	8.3
22	"	"	"	"	"	"	2.01	5.9
33	2.83	3.4	1.06	10.8	5.02	5.0	2.36	6.2
44	0.66	-0.2	0.58	2.7	1.47	2.2	0.67	2.1
55	"	"	"	"	"	"	0.81	1.7
66	0.90	0.3	0.40	-2.7	1.68	1.5	0.81	2.3
12	1.29	3.9	0.07	8.7	1.63	3.3	0.07	4.3
13	1.19	3.3	0.12	6.0	1.17	3.7	0.07	4.2
23	"	"	"	"	"	"	0.07	3.5
14	-	-	-0.18	1.9	-0.23	0.1	-	-

Reference Yoon, 1971

McSkimin,
Andreatch &
Thurston,
1965

Gieske and
Barsch,
1968

Graham and
Barsch, 1969

A rough value for $\Delta k/\Delta \ell$ can be obtained by examining how k varies with interatomic distance. Short strong bonds have larger stiffnesses than long bonds. The bond stiffness for Si-O is about 10% larger than that for Al-O, and the bond length is about 10% shorter. Therefore $\Delta k/\Delta \ell$ is roughly $-2 \text{ md}/\text{\AA}^2$.

Stretching force constants are plotted as a function of interatomic distance in Fig. 2. For distances greater than 1.5\AA , the relation between k and ℓ is nearly linear with a slope of about $-2 \text{ md}/\text{\AA}^2$.

Substituting this value in (4) along with $c = 3 \times 10^{12} \text{ dyne/cm}^2$, $k = 1 \text{ md}/\text{\AA}$ and $\ell = 3\text{\AA}$ gives $\Delta c/\Delta P \sim 10$ (dimensionless), the right order of magnitude.

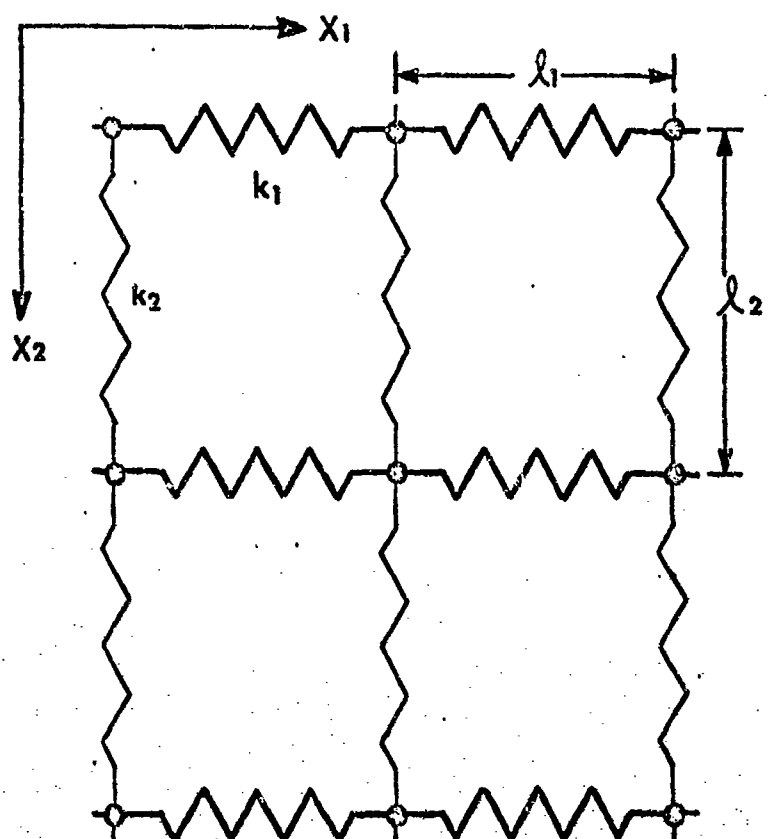
To explain the second observation consider the anisotropic structure in Fig. 5a. The structure contains tightly bonded atoms in the X_1 direction and very loose bonding along X_2 . From arguments previously presented $c_{11} > c_{22}$. Now consider their pressure derivatives. From eq. (3) the change in stiffness with pressure is related to the change in the number of chains per unit area n/A , their repeat distance ℓ , and bond stiffness k :

$$\frac{\Delta c}{\Delta P} = \ell k \frac{\Delta(n/A)}{\Delta P} + \frac{n k}{A} \frac{\Delta \ell}{\Delta P} + \frac{n \ell}{A} \frac{\Delta k}{\Delta P} \quad (5)$$

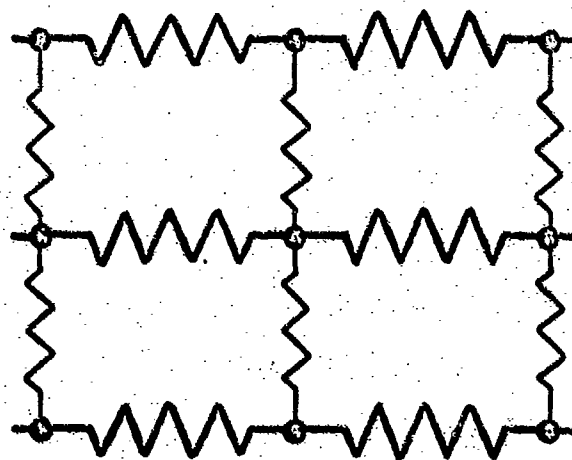
Under pressure the structure will compress mainly along X_2 because of the weak bonding in that direction, giving the exaggerated deformation in Fig. 5b.

For the X_1 direction there will be little change in ℓ_1 and k_1 so that $(\Delta c_{11}/\Delta P) \sim \ell_1 k_1 \Delta(n/A)/\Delta P$. The number of chains per unit area increases rapidly with pressure because of the big reduction in ℓ_2 , decreasing A and increasing n/A . Therefore c_{11} increases rapidly with pressure.

Fig. 5. Anisotropic model at low (a) and high (b) pressures.



(a)



(b)

For direction X_2 , there is little change in n/A with pressure because ℓ_1 hardly changes. Therefore $\Delta c_{22} / \Delta P \approx (n/A) [k_2 (\Delta \ell_2 / \Delta P) + \ell_2 \Delta k_2 / \Delta P]$. The length and spring constant are inversely related to one another so that the increase in spring constant is partially offset by change in length. Hence c_{22} will not increase rapidly with pressure.

The third observation regarding the pressure dependence is the occurrence of negative derivatives in open structures like beryl and quartz. When a close-packed structure is compressed, the atoms move closer together but this need not be true in an open structure where rotations can take place. To determine the effect on the elastic constants, consider equation (5) describing the pressure dependence of the stiffness. The new feature here is the pressure dependence of the stiffness k . If we are considering the stiffness along X_1 , for example, k_1 may decrease with P because at high pressure a stress along X_1 produces a bending rather than a stretching motion. The stiffness coefficients for bending are considerably smaller than for stretching. Thus rotation can lead to negative pressure dependence of shearing stiffness coefficients.

Temperature dependence of the elastic stiffness

Most materials soften as they become warmer, so that the elastic stiffness decreases as temperature increases. Some representative values of dc/dT for oxides are given in Table 3. The fractional change in stiffness $(1/c) (dc/dT)$ is of the order -2×10^{-4} per $^{\circ}\text{C}$. The variation of the elastic coefficients with temperature is of some geophysical interest because of the increase in temperature with depth. Stiffness increases with pressure so that acoustic waves increase speed with depth, but the increase is partly offset by the temperature effect. The temperature dependence of the elastic constants is also important

Table 3. Temperature coefficients of elastic stiffness for several oxides.

$T_c = (1/c)(dc/dT)$ and is expressed in units of 10^{-4} per $^{\circ}\text{C}$.

MgO	$T_{c_{11}} = -2.3$	$T_{c_{44}} = -1.0$
SrTiO_3	$T_{c_{11}} = -2.6$	$T_{c_{44}} = -1.1$
αSiO_2	$T_{c_{11}} = -0.5$	$T_{c_{33}} = -2.1$
	$T_{c_{44}} = -1.6$	$T_{c_{66}} = +1.6$

in acoustic delay lines and in piezoelectric oscillators and filters. Variations of the delay time or resonant frequencies are undesirable in these devices.

The mechanical spring model just discussed also provides an explanation of the temperature dependence of the elastic stiffness. To estimate the size of dc/dT , we assume an isotropic model of identical springs, for which $c = n \ell k/A = k/\ell$, as shown previously. k is the force constant of the spring and ℓ the length. The temperature derivative is

$$\frac{dc}{dT} = \frac{d}{dT} \left(\frac{k}{\ell} \right) = \frac{1}{\ell} \frac{dk}{dT} - \frac{k}{\ell^2} \frac{d\ell}{dT}.$$

The second term is directly proportional to the linear thermal expansion coefficient $\alpha = (1/\ell) (d\ell/dT)$. The first term depends on the change in force constant with temperature. Chemical bonds grow weaker with increasing length and the force constant becomes smaller. If we assume that the change in k depends primarily on ℓ , then $(dk/dT) = (dk/d\ell)(d\ell/dT)$, and the variation stiffness with temperature becomes:

$$\frac{dc}{dT} = \alpha \frac{dk}{d\ell} - \frac{k}{\ell} \alpha.$$

As shown in the previous section, $dk/d\ell \sim -2 \text{ md/\AA}^2$, $k \sim 1 \text{ md/\AA}$, $\ell \sim 3\text{\AA}$, and $c \sim 3 \times 10^{12} \text{ dynes/cm}^2$. Thermal expansion coefficients for oxides are about 10^{-5} per $^{\circ}\text{C}$.

Substituting these values gives a fractional change $(1/c)(dc/dT) \sim 10^{-4}/^{\circ}\text{C}$, which is the right order of magnitude. This value is small, but is several times larger than the thermal expansion coefficient α . This is important because the thermal expansion coefficients are crucial in delay line and frequency-standard devices. Thus in searching for zero-temperature coefficients, materials with unusual elastic properties are needed. In particular, it is important to find materials with positive temperature coefficients $(1/c)(dc/dT)$. In the next section we consider the circumstances under which this might occur.

Temperature - Compensated Materials

The transit time t in a delay-line medium is given by the transit distance ℓ divided by the acoustic velocity $\sqrt{c/\rho}$. c is the appropriate stiffness coefficient and ρ the density. Temperature variations alter the transit time, causing problems. The temperature derivative $(1/t)(dt/dT) = (1/\ell)(d\ell/dT) - (1/2 c)(dc/dT) + (1/2 \rho)(d\rho/dT)$. The first term on the right is the linear thermal expansion coefficient α , measured parallel to the transit direction. The third term is also related to α . For an isotropic material, $(1/\rho)(d\rho/dT) = -3\alpha$. Thus the temperature drift of the delay time is governed by the thermal expansion coefficients and by the change in stiffness with temperature:

$$T_c = (1/t)(dt/dT) \approx -1/2(\alpha + T_c).$$

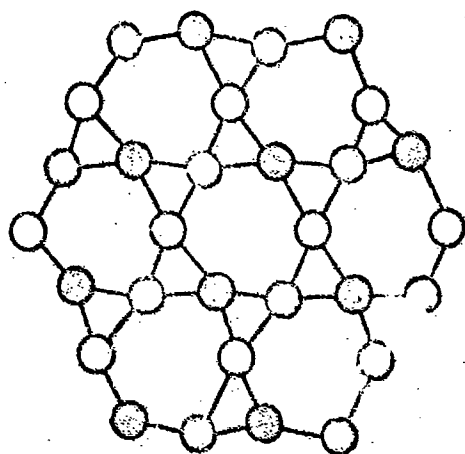
T_c is $(1/c)(dc/dT)$, the fractional change in stiffness coefficient with temperature, and is approximately $-2 \times 10^{-4}/^\circ\text{C}$, as discussed in the previous section. Thermal expansion coefficients are usually positive and somewhat smaller, about $+10^{-5}/^\circ\text{C}$. The temperature variation of the transit time is therefore determined by T_c , and is about $10^{-4}/^\circ\text{C}$. Observed values of T_c reported for surface wave devices are slightly smaller, about 30-90 ppm/ $^\circ\text{C}$ (Carr, 1972).

Temperature-compensation requires that T_c , the temperature coefficient of the transit time, be zero. For most materials, T_c is positive because elastic stiffness decreases with increasing temperature, slowing down the acoustic waves and lengthening the transit time. Density also decreases with temperature, speeding up the waves and shortening the transit time, but this effect is generally smaller than that due to the elastic constants.

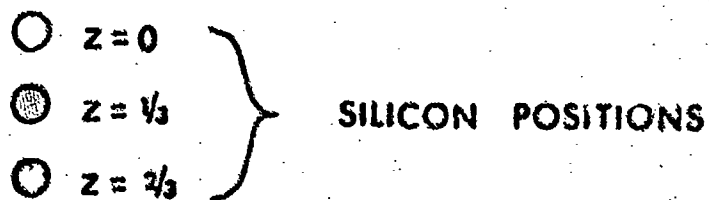
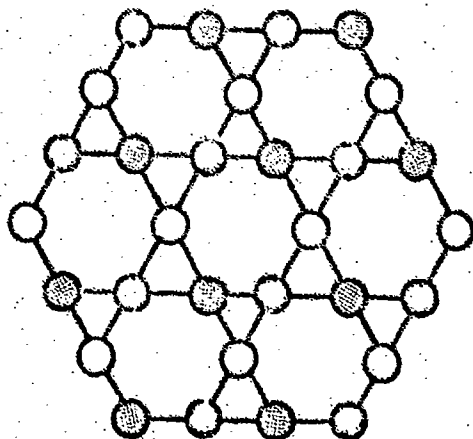
Materials with unusual values of T_c are therefore of special interest for temperature-compensated devices. Quartz is such material since T_c for shear about the z -axis is positive (Table 3). The structures of α and β -quartz (Fig. 6.) provide an understanding of this behavior. The α -quartz structure is a partially-collapsed derivative of β -quartz. At higher temperatures the SiO_4 tetrahedra

Fig. 6. Arrangement of silicon atoms in quartz. Oxygens are located approximately midway between neighboring silicon atoms.

α - QUARTZ



β - QUARTZ



rotate to an open, fully-expanded structure, undergoing a displacive phase transition at 573°C to the β -quartz structure. Quartz shows a rather high rate of thermal expansion at room temperature due to the rotation of the tetrahedra.

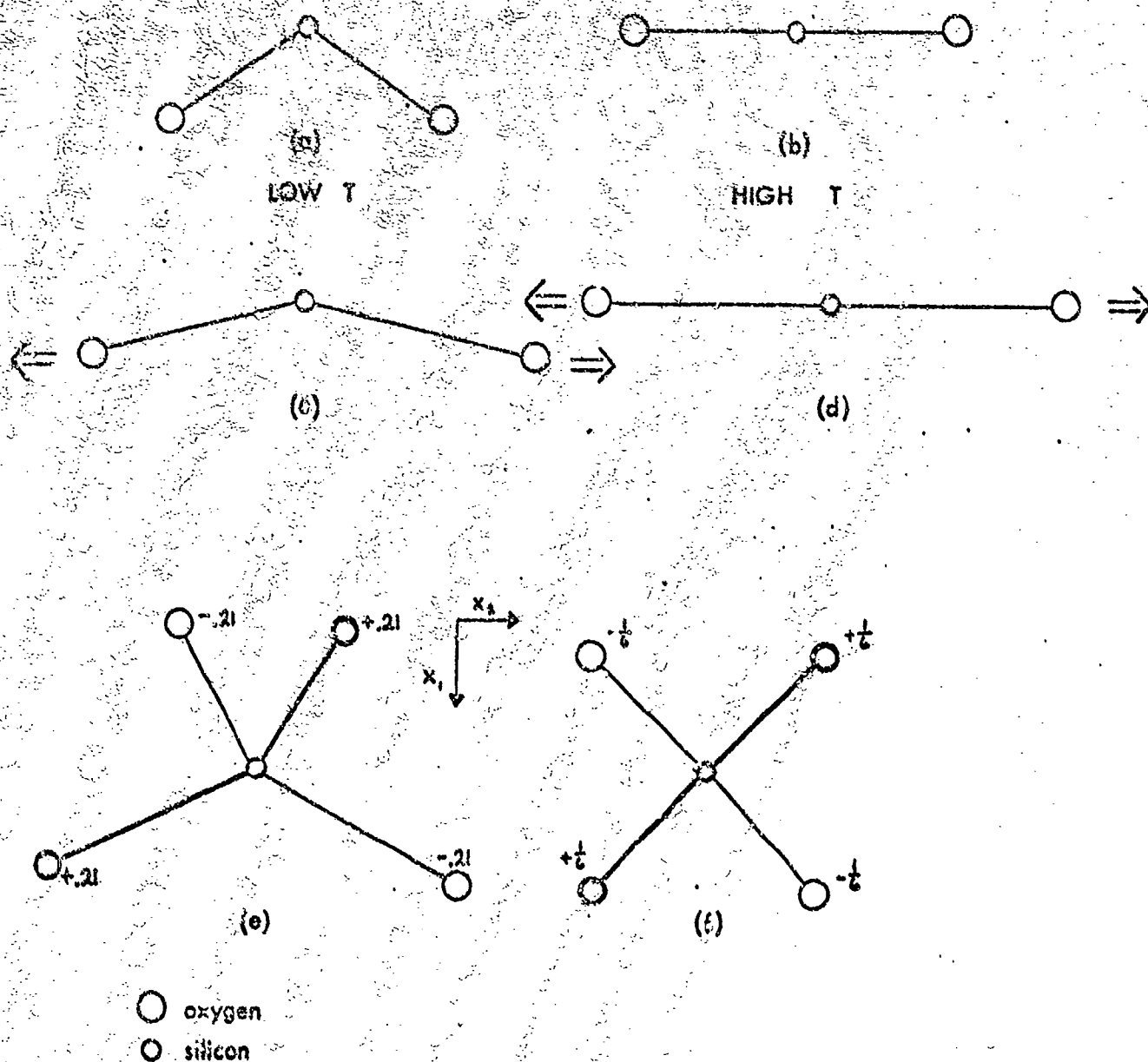
Thermal expansion coefficients become even larger just below the transformation temperature and then decrease abruptly to near zero when the fully-expanded structure is achieved. Quantitative calculations (Taylor, 1972), show that the thermal expansion of quartz is due chiefly to tetrahedral rotations, with only a minor contribution from thermal motion. The anomalous value of T_{c66} is related to the rotation effect. c_{66} relates a shearing stress about the z-axis to a shearing strain about the same axis - the same type of motion involved in the rotation of tetrahedra in transforming from α to β quartz. At room temperature the Si - O - Si bonds are quite bent, (Fig. 7a), but they straighten with increasing temperature (Fig. 7b) as the structure grows closer to β -quartz. Consider the effect of mechanical stress on such arrangements. When the bent structure is stretched, the tetrahedra rotate as well as deform (Fig. 7c), resulting in a sizeable strain. Thus the stiffness is rather small at room temperature. When the high-temperature structure is stressed (Fig. 7d), only deformation occurs since the structure is too straight to permit rotation. As a result, there is less strain and the stiffness increases with temperature. A positive value of T_c can be related to rotational effects in this way.

In an earlier section, the temperature coefficient of the elastic stiffness c was described in terms of a mechanical spring model. There it was shown that

$$T_c = (1/c)(dc/dT) = (1/lc)(dk/dT) - (k/l^2c)(dl/dT).$$

In this equation, l is the length of the spring and k is the spring constant. For most materials, T_c is determined by the first term on the right, resulting from the change in spring constant with temperature. The second term arises from thermal expansion, and is generally smaller. The spring constant usually decreases with temperature because of thermal vibrations, so that dk/dT is usually negative and so is T_c .

Fig. 7. Models indicating the origin of positive T_c coefficients in open crystal structures. (a) shows three atoms connected by bent bonds. At higher temperatures (b) the bond straightens. When stressed, the bent bonds both lengthen and rotate, as shown in (c). When the straight bonds are stressed, only lengthening takes place (d). (c) shows a larger overall change in length than (d), hence the low-temperature structure is more compliant. The bent bonds in α -quartz are shown in (e). A shearing stress about X_3 produces tension along the bond direction, resulting in bond rotation as well as extension. For the high-temperature β -quartz structure (f), no bending occurs in this projection.

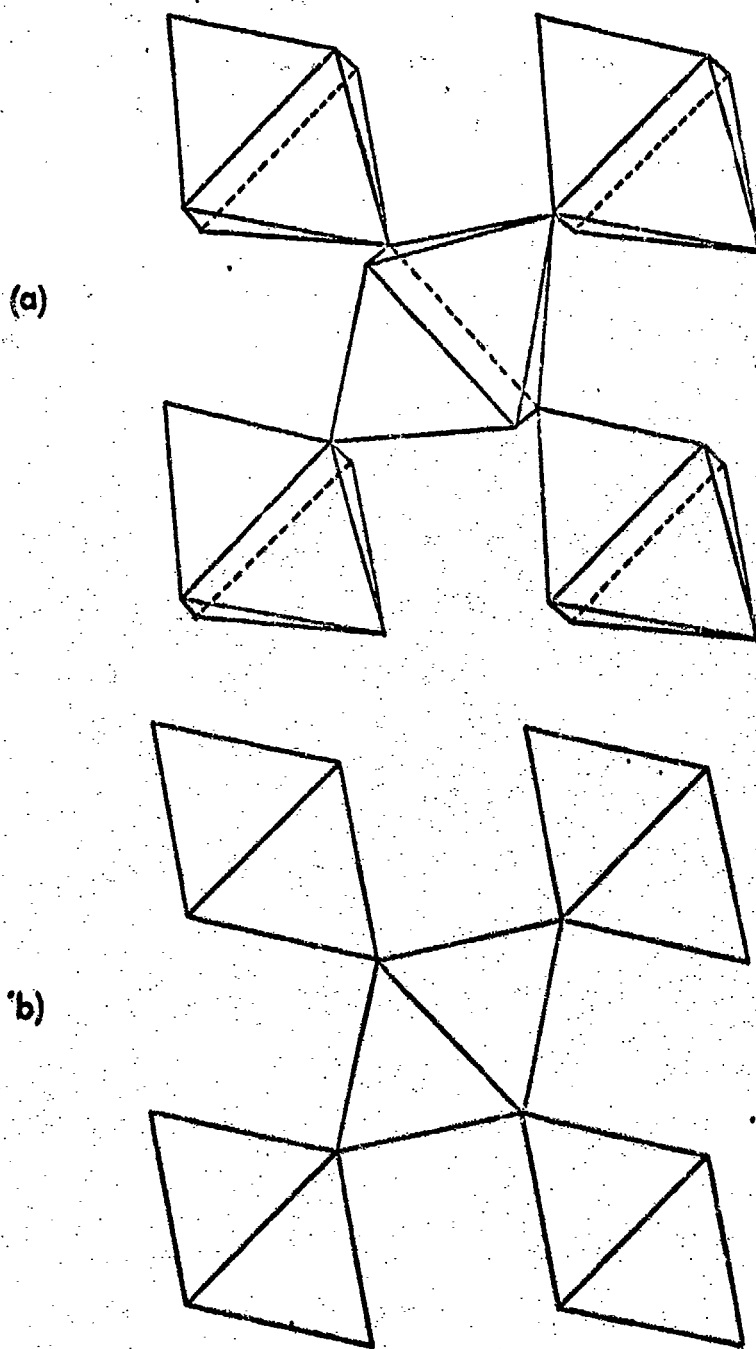


This need not be so when rotations occur because rotational spring constants are smaller than stretching spring constants. For Si-O bonds, the stretching constant is about $5 \text{ md}/\text{\AA}$ while bending spring constants are less than $1 \text{ md}/\text{\AA}$. In the kinked bonds (Fig. 6a) both stretching and bending occurs under stress (Fig. 7c). The effective force constant is smaller than in the high-temperature case (Figs. 7b and 7d) where only stretching takes place. In this situation dk/dT is positive, as is T_c , because the force constant changes character with increasing temperature.

Paratellurite, one of the polymorphs of tellurium dioxide, exhibits unusual elastic behavior similar to quartz. Temperature-compensated cuts of paratellurite have been used in surface wave devices, although the piezoelectric coupling parameters are small (Carr, 1972). In TeO_2 the shearing stiffness $c_s = 1/2 (c_{11} - c_{12})$ has a positive temperature coefficient. The crystal structures of the paratellurite and rutile polymorphs of TeO_2 are illustrated in Fig. 8. Paratellurite is a partially-collapsed derivative of the rutile form. When paratellurite is heated, the bent configuration straightens, similar to the changes observed in quartz. Thus the shearing spring constant increases with temperature making dc/dT positive.

In searching for new materials with positive temperature coefficients, we look to open structures in which sizeable rotations can occur. Coordination numbers are usually small in open structures, so that oxygens are bonded to only 1, 2, or 3 neighbors. Close-packed structures are generally not conducive to rotational movements, although there are exceptions to this. SrTiO_3 shows a beautiful rotational transition near 110°K which is accompanied by anomalous elastic behavior. The Ti-O-Ti bonds are kinked in the low-temperature structure. Leucite, cristobalite, anorthite, and other silicate minerals show 'puckering' transitions similar to quartz but unfortunately these materials are not piezoelectric.

Fig. 8. Crystal structures of paratellurite (a) and rutile (b) viewed along the c crystallographic axes. The tilting of the TeO_6 octahedra in paratellurite leads to bond-bending and anomalous elastic behavior.



Phase transitions are a second clue to the occurrence of positive T_c values, since rotations sometimes lead to a change in structure. 'Poled' ferroelectrics such as LiTaO_3 or ferroelastics are therefore of interest. To prevent domain formation, the transition should not be near room temperature. A material such as Bi_2WO_6 ($T_c = 950^\circ\text{C}$) might be of interest. The elastic constants of bismuth tungstates have not been determined. Bi_2WO_6 is polar at room temperature but not ferroelectric. Like lithium niobate, it is a 'frozen' ferroelectric.

Anomalous elastic properties are also observed in $\text{Ba}_2\text{NaNb}_5\text{O}_{15}$, known colloquially as bananas. The compliance coefficients s_{44} and s_{55} decrease with increasing temperature (Yamada, Iwasaki and Niizeki, 1970). As with SiO_2 and TeO_2 , the unusual behavior is associated with a phase transition to higher symmetry. Barium sodium niobate undergoes a displacive phase transition at 300°C which is primarily elastic in character. The x and y axes of the room-temperature orthorhombic structure are rotated by 45° from those of the high-temperature tetragonal phase. $\text{Ba}_2\text{NaNb}_5\text{O}_{15}$ exhibits large piezoelectric coupling constants in certain directions.

REFERENCES

- ANDERSON (O.L.) and NAPE (J.E.), 1965. J. Geophys. Res., Vol. 70, p. 3951.
- BIRCH (F.), 1961a. J. Geophys. Res., Vol. 66, p. 295.
- BIRCH (F.), 1961b. J. Geophys. Res., Vol. 66, p. 2199.
- BRAGG (W.L.), 1924. Proc. Roy. Soc., Vol. A105, p. 370.
- CARR (P.H.), 1972. I.E.E.E. Trans. SU-19 357.
- GIESKE (J.H.), and BARSCH (G.R.), 1968. phys. stat. solidi, Vol. 29, p. 121.
- GRAHAM (E.K.), and BARSCH (G.R.), 1969. J. Geophys. Res., Vol. 75, p. 5949.
- HEARMON (R.F.S.), 1966. Landolt-Börnstein Tables, Group III, Vol. I, Springer, Berlin.
- HIDALGO (A.), and SERRATOSA (J.M.), 1956. Chem. Abstr., Vol. 50, p. 10532gh.
- KITTEL (C.), 1953. Introduction to Solid State Physics, John Wiley & Sons, N.Y., p. 53.
- MATOSI (F.), 1949. J. Chem. Phys., Vol. 17, p. 679.
- MCSKININ (H.J.), ANDREATCH (P.), and THURSTON (R.N.), 1965. J. Appl. Phys., Vol. 36, p. 1524.
- NYE (J.F.), 1957. Physical Properties of Crystals, Oxford University Press, London. Chapter VIII.
- SIMMONS (G.), 1964. J. Geophys. Res., Vol. 69, p. 1123.
- SUTTON (L. E.), 1958. Tables of Interatomic Distances and Configuration in Molecules and Ions, Special Publication No. 11, The Chemical Society, London.
- TAYLOR (D.), 1972. Min. Mag. 38 593
- WILSON (E.B.), DECIUS (J.C.), and CROSS (P.C.), 1955. Molecular Vibrations, McGraw-Hill Book Co., N.Y., p. 175.
- YAMADA (T.), IWASAKI (H.), and NIIZEKI (N.), Elastic Anomaly of Ba₂Nb₂O₇ 15. J. Appl. Phys. 41 (10), 4141-4147 (1970).
- YOON (H.S.), 1971. Ph.D. Thesis, The Pennsylvania State University.

ACKNOWLEDGEMENTS

The section on elastic anisotropy in minerals was written previously for Contract No. DA-19-066-AMC-325(X) sponsored by the Army Materials and Mechanics Research Center. We also wish to thank Prof. G. R. Barsch, Prof. L. E. Cross, Dr. H. S. Yoon, and Dr. Paul Carr for helpful suggestions.